Soft Matter

REVIEW

Cite this: *Soft Matter*, 2018, **14**, 3669

A review of Winkler's foundation and its profound influence on adhesion and soft matter applications

David A. Dillard, *[a] Bikramjit Mukherjee, [b] Preetika Karnal, [c] Romesh C. Batra [a] and Joelle Frechette [c]

Received 19th October 2017,
Accepted 10th April 2018

DOI: 10.1039/c7sm02062g

rsc.li/soft-matter-journal

Few advanced mechanics of materials solutions have found broader and more enduring applications than Emil Winkler's beam on elastic foundation analysis, first published in 1867. Now, 150 years after its introduction, this concept continues to enjoy widespread use in its original application field of civil engineering, and has also had a profound effect on the field of adhesion mechanics, including for soft matter adhesion phenomena. A review of the model is presented with a focus on applications to adhesion science, highlighting classical works that utilize the model as well as recent usages that extend its scope. The special case of the behavior of plates on incompressible (*e.g.*, elastomeric and viscous liquid) foundations is reviewed because of the significant relevance to the behavior of soft matter interlayers between one or more flexible adherends.

1. Introduction

Peel stresses, those normal stresses perpendicular to the adhesive layer or bond plane, have long been considered the nemesis of adhesive bonds and a dominant cause of debonding for other adhesion phenomena. These opening mode stresses tend to pull bonds apart and prevent opportunities for rebonding, as can occur when shear or sliding takes place at soft material interfaces. Associated with mode I fracture, which is often

[a] *Biomedical Engineering and Mechanics Department, Virginia Polytechnic Institute and State University, Blacksburg, Virginia, 24061, USA. E-mail: dillard@vt.edu; Tel: +1-540-231-4714*
[b] *The Dow Chemical Company, Lake Jackson, TX 77566, USA*
[c] *Department of Chemical and Biomolecular Engineering and Hopkins Extreme Materials Institute, Johns Hopkins University, Baltimore, Maryland, 21218, USA*

David A. Dillard

David Dillard is the Adhesive and Sealant Science Professor in the Biomedical Engineering and Mechanics Department at Virginia Tech. With broad experience across a range of adhesion phenomena, his research often involves using the principles of fracture mechanics and viscoelasticity to develop test methods and predictive models for understanding and estimating the performance and durability of polymeric materials, adhesives, and bonded joints. Active in the Adhesion Society, he is a Patrick Fellow, past president, and 2010 recipient of their Award for Excellence in Adhesion Science. An ASME Fellow, he received the Society for Adhesion and Adhesives' 2013 Wake Memorial Medal.

Bikramjit Mukherjee

Bikramjit Mukherjee is a Sr Engineer in Plastics Characterization and Testing R&D of The Dow Chemical Company in Lake Jackson, TX. He earned his PhD in Engineering Mechanics in Fall, 2016 from Virginia Tech under the supervision of Prof. Romesh C. Batra and Prof. David A. Dillard. His research interests include mechanics of adhesion, fracture mechanics and mechanical characterization of polyolefin materials. He earned his Bachelor's in Mechanical Engineering from Jadavpur University, Kolkata, India in 2009.

considered to require the smallest energy release rates for failure in monolithic and layered systems, peeling action opens pathways for moisture ingression and can facilitate penetration of other materials that reduce adhesion or otherwise degrade bonded systems. Perhaps no closed-form, mechanics of materials solution has had more impact on the field of adhesion and adhesive bonding than the understanding obtained when peel stresses are assessed by assuming adherend beams (or plates) are supported by an elastic foundation associated with the adhesive interlayer. Originally proposed for civil engineering applications, Winkler's beam (and by extension, plate) on elastic foundation solution has proven invaluable for myriad applications including tubular structures, hydrostatic support of floating plates, and adhesive bonds. Adhesion-related solutions include assessing peel stresses within lap joint configurations, peeling of pressure sensitive tapes, and fracture of laminated material systems. When appropriately modified to account for foundation incompressibility, this solution can accurately be extended to situations involving a viscous liquid or a soft elastomer. These modifications have been widely employed in modeling soft matter adhesion phenomena including cavitation and fingering instabilities, patterned adhesion, removal of plates from viscous liquids, and debonding behavior in biological and biomimetic problems.

2017 marked the 150th anniversary of Emil Winkler's seminal publication of the beam on elastic foundation (BoEF) solution,[1] published in 1867 while he was a professor at the University of Prague. With wide-ranging interests in analysis of civil engineering structures, he initially proposed the BoEF model for the rather obvious application to sleepers and rails supported by the earth upon which they rest.[2] The essence of the model lies in the simple but profound assumption that the restoring force, q, of an elastic foundation is linearly proportional to the deflection w it sustains, according to $q = kw$. The important resulting mechanics of materials solution has been applied to a wide range of engineering problems, including a plethora of discrete and continuous loading and boundary conditions, extensions to plates and pontoon bridges, and nonlinear behavior. The analysis has even been extended to determine deflections and stresses in pressurized cylindrical tanks, where the effective restoring force is not supplied by a separate medium but rather by the hoop stresses developed due to stretching of the curved walls.[3] Although variational forms will be discussed briefly in a subsequent section, the equilibrium formulation for an Euler–Bernoulli beam (illustrated in Fig. 1a and b) results in a governing differential equation (GDE) and the characteristic reciprocal length λ_w of

$$\frac{d^4w}{dx^4} = \frac{p-q}{EI} \Rightarrow \frac{d^4w}{dx^4} + 4{\lambda_w}^4 w = \frac{p}{EI}$$
$$\lambda_w = \sqrt[4]{\frac{k}{4EI}} \quad (1)$$

Preetika Karnal

Preetika Karnal received her bachelor's degree in Chemical Engineering Department in Indian Institute of Technology, Bombay in India. She is currently a PhD candidate in the Chemical and Biomolecular Engineering Department at Johns Hopkins University. Her research focus is on investigation of the significance of surface properties of acrylic pressure sensitive adhesives.

Romesh C. Batra

Romesh Batra, Clifton Garvin Professor at Virginia Tech, has mentored 37 (34 solo) PhD, 19 MSc and 62 Post-doctoral Fellows/visitors. His group has published in reputable peer-reviewed journals 425 papers including 40 single-authored and 300 two-authored that have received 16 150 citations with H-index = 67 on google.scholar (H = 56 on Scopus). His book "Elements of Continuum Mechanics" has been widely adopted. His honors include 2016 ASME Robert Henry Thurston Lecture Award, 2015 ASME Honorary Membership, 2011 Virginia Outstanding Scientist Award, 2010 Virginia Outstanding Faculty Award, and the 2006 Engineering Science Medal from the Society of Engineering Science.

Joelle Frechette

Joelle Frechette is an associate professor of Chemical & Biomolecular Engineering at Johns Hopkins University. She received her PhD from Princeton University in 2005. She joined Johns Hopkins University in 2006 after a post-doctoral appointment at the University of California, Berkeley. Her research interests span colloid and interfacial science, wetting and adhesion.

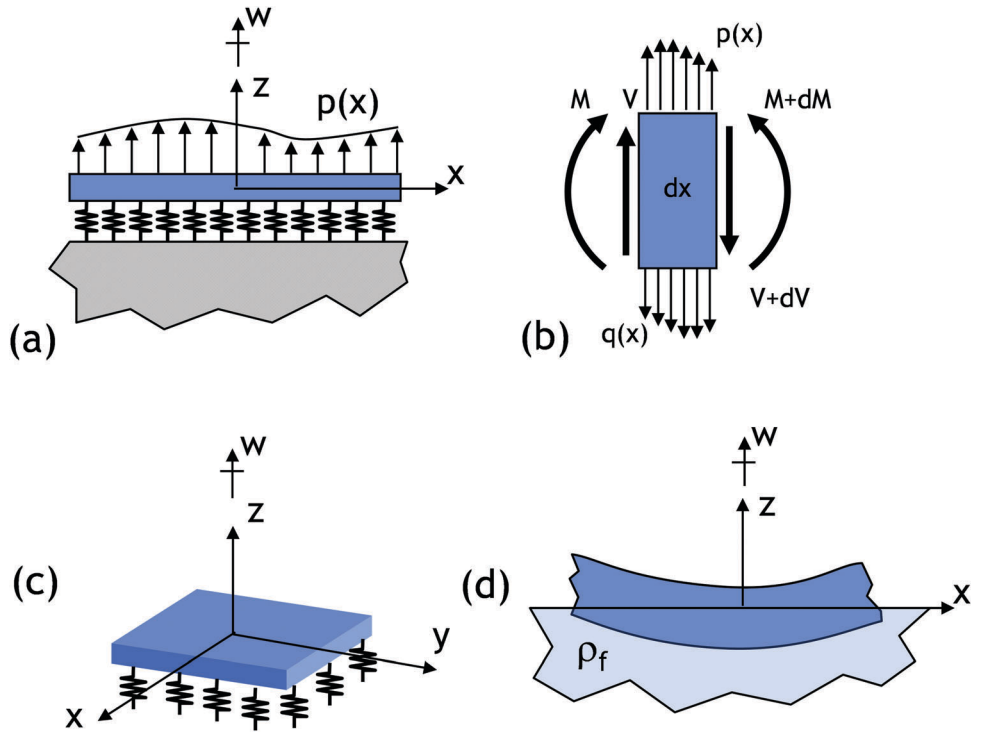

Fig. 1 Illustrations of configurations and sign conventions for: (a) simple beam on elastic foundation subjected to lateral loading, (b) free body diagram of a differential beam element including moment M and transverse shear V, (c) plate on elastic foundation, and (d) plate supported by a liquid of density ρ_f.

where w is also the beam deflection, p is the applied (per unit length along beam) lateral loading,† E and I are, respectively, Young's modulus and second moment of area of the beam about its neutral axis, and k is the elastic foundation stiffness (force per unit displacement per unit length of beam).

The complimentary solution of the GDE involves exponentially varying, sinusoidal undulations of the form:

$$w(x) = C_1 e^{-\lambda_w x}\cos\lambda_w x + C_2 e^{-\lambda_w x}\sin\lambda_w x + C_3 e^{\lambda_w x}\cos\lambda_w x + C_4 e^{\lambda_w x}\sin\lambda_w x \quad (2)$$

where C_1, C_2, C_3, and C_4 are the integration constants determined from problem-specific boundary and/or continuity conditions. As can be seen in its definition given above, the characteristic length scale λ_w^{-1} represents the deformability of the foundation relative to that of the beam. As one can see from (2), the reciprocal length governs the decay rate (from the point of load application) and the period of the oscillations. It corresponds to the exponential decay length in a similar manner that the shear lag distance is defined in the Volkersen solution.[4] The rapid decay rate relative to the oscillation period means that the oscillations become negligible after several characteristic lengths; $5\lambda_w^{-1}$ is the traditional definition of a "short beam" for BoEF solutions.[5] It is tacitly assumed here that, during the deformation process, there is no separation between the deformed beam and the foundation and that neighboring particles of the foundation deform independently of each other. Furthermore, the bending-induced axial displacements at the beam surface are neglected in the Winkler formulation (and most extensions, including all those discussed herein).

From its introduction, Winkler's BoEF approach found widespread applications as well as numerous extensions. Biot[6] took exception with Winkler's solution in 1937, arguing that the foundation model applicability was rather limited, effectively because it applied to a layered system (beam atop a foundation layer atop a rigid substrate). Biot's interesting development extended the solution to the case where the foundation is a half-space and the applied load is sinusoidal, resulting in a foundation stiffness that effectively became a function of the spatial frequency of the applied load. His analysis would later find widespread applications for surface layer wrinkling analysis, where the surface layer thickness is small compared to that of the underlying material.

Hetényi[3] presented solutions for a very wide range of BoEF geometries and loading cases, including applications to cylindrical pressure vessels, torsion, and buckling, in his classic 1946 monograph. Apparently largely based on his dissertation and *postdoc* tenure with Timoshenko a decade earlier, this source remains a thorough and seminal work illustrating some of the many outcomes of Winkler's foundation predictions.

Winkler's foundation is easily extended to a generalized formulation for plates (shown in Fig. 1c) by using a similar, spatially varying restoring force (per unit area): $\nabla^4 w = (p - q)/D$,

† Note that here and elsewhere throughout the paper, p is the externally applied mechanical loading. The zero deflection reference state is assumed to coincide with any deflection resulting after the linear (for beam) or areal (for plate) self weight is applied.

where $D = Et_p^3/12(1 - \nu_p^2)$ is the plate bending rigidity, with modulus of E, Poisson's ratio of ν_p and thickness t_p, $\nabla^4 w = \nabla^2(\nabla^2 w)$ and $\nabla^2 = \frac{\partial^2}{\partial x^2} + \frac{\partial^2}{\partial y^2}$. (Note that in moving from beam to plate solutions, as covered in remainder of the paper, p, q, and k all are per unit area rather than per unit length.) Again, making the Winkler assumption that $q = kw$ results in:

$$\nabla^4 w + 4\lambda_w^4 w = \frac{p}{D}$$
$$\lambda_w = \sqrt[4]{\frac{k}{4D}} \quad (3)$$

To avoid plate stretching due to Gaussian curvature changes, we re-emphasize the need for small displacements ($w < t$) and initially flat plates. Assuming that a point on the foundation deforms independently of its neighbors, the foundation stiffness may be taken as $k = E_a/h$, where E_a is Young's modulus‡ of the foundation (or adhesive interlayer, as will be important in much of the paper) and h is its thickness. According to Timoshenko and Woinowsky-Krieger,[7] early contributions to the plate solution and applications are due to Hertz[8,9] and Föppl,[10] and also note that Hertz's analysis was for a floating plate, where the spring constant results not from an elastic property, but rather from the hydrostatic pressure based on the weight of the displaced liquid column upon which it rests. In a generalized form the hydrostatic forces are incorporated, resulting in the same GDE as in (3), but with $k = \rho_f g$, where ρ_f is the density of the liquid, and g is gravitational acceleration, as illustrated in Fig. 1d.

Plane strain (cylindrical, or plane stress of narrow beam) bending has been widely analyzed and is commonly used in experiments reported in the literature, including for adhesion applications, so will be the focus of this paper. This avoids changes in Gaussian curvature and concomitant stretching; the GDE simplifies to:

$$\frac{d^4 w}{dx^4} + 4\lambda_w^4 w = \frac{p}{D} \quad (4)$$

The remainder of the paper will build on this background, reviewing in Section 2 some classical and recent applications of the BoEF to the predictions of stresses within adhesive bonds and layered systems, and to modeling fracture within beam-like monolithic and layered specimens. With particular interest in the modifications required to adapt the BoEF approach to situations involving soft matter interlayers, including elastomers and fluids where coupling effects become important, we then briefly review the history of BoEF modifications involving other classic coupling effects in Section 3. The development and applications of the modified BoEF solution for soft matter interlayers is presented in Section 4, where interlayer incompressibility dictates a specific form of coupling resulting in 6th order rather than 4th order GDEs, contrasting their differences on the predicted stress fields. Section 5 then outlines the analogous solution including hydrostatic and hydrodynamic contributions for viscous fluids. Prior to the Conclusion, Section 6 summarizes the key solutions presented, and adds assumptions and requirements for key equations. Throughout the manuscript, numerous applications to soft elastomer and viscous fluids are both included, with relevance to pressure sensitive adhesives, soft gel adhesion, release technology, a range of biological adhesion phenomena, and biomimetic configurations.

‡ Note that the symbol E is used throughout the paper to denote Young's modulus of the adherend beam/plate whereas E_a is used to denote Young's modulus of the foundation/adhesive layer. However the subscript 'a' is not used in the symbols of the shear modulus (μ) and Poisson's ratio (ν) of the foundation layer.

2. Applications to adhesion

Of particular interest to the adhesion community has been the varied adaptations of Winkler's model to the field of adhesion, where it ranks with Volkersen's 1938 shear lag model[4] in both importance and versatility in modeling and explaining stress states in bonded systems. The long list of applications of the Winkler foundation to adhesion apparently began with Goland and Reissner's 1944 analysis[11] of the stresses within single lap joints, in which they recognized the significant influence that adherend bending, associated with eccentric loading, imposed on the resulting stress state within the bondline. Considering the adhesive layer as relatively more extensible in the out of plane direction than the adherends, the adhesive layer was effectively modelled as an elastic foundation supporting the two adherends. The assumption is analogous to that of the shear lag model, which they incorporated for assessing the shear stress distribution. In spite of the simplifying assumptions made, Goland and Reissner's model combining shear lag and BoEF effects accurately predicts the bondline shear and peel stresses for a range of practical adhesive joints, often closely matching more sophisticated analytical or numerical solutions for common joint configurations. In 1956 Lubkin and Reissner[12] extended this lap joint analysis to tubular lap joints, augmenting the adhesive foundation stiffness with the radial constraint provided by circumferential stretching of the cylindrical tubes, as noted earlier.[3] Other direct applications of the BoEF model include the more recent analysis of stresses between adherends with a curvature mismatch, including constant[13] and varying[14] mismatch cases, as well as curvature optimization to minimize detrimental peel stresses and edge lift.[15] In all of these analyses, the foundation stiffness is assumed to be based on that of the adhesive interlayer, which is typically of the same width as the adherends, but can also be narrower, with appropriate stiffness scaling.

Extensions of the BoEF concept to debonding and fracture mechanics applications, including the above mentioned analyses, can be easily accomplished by effectively shortening the foundation-supported length and extending the debonded adherend length (see Fig. 2). Such self-similar or steady state fracture analyses have found wide applications in modeling the stresses ahead of a growing crack or debond, such as appear in Spies' 1953 classic analysis of peeling tests,[16] in Bikerman's

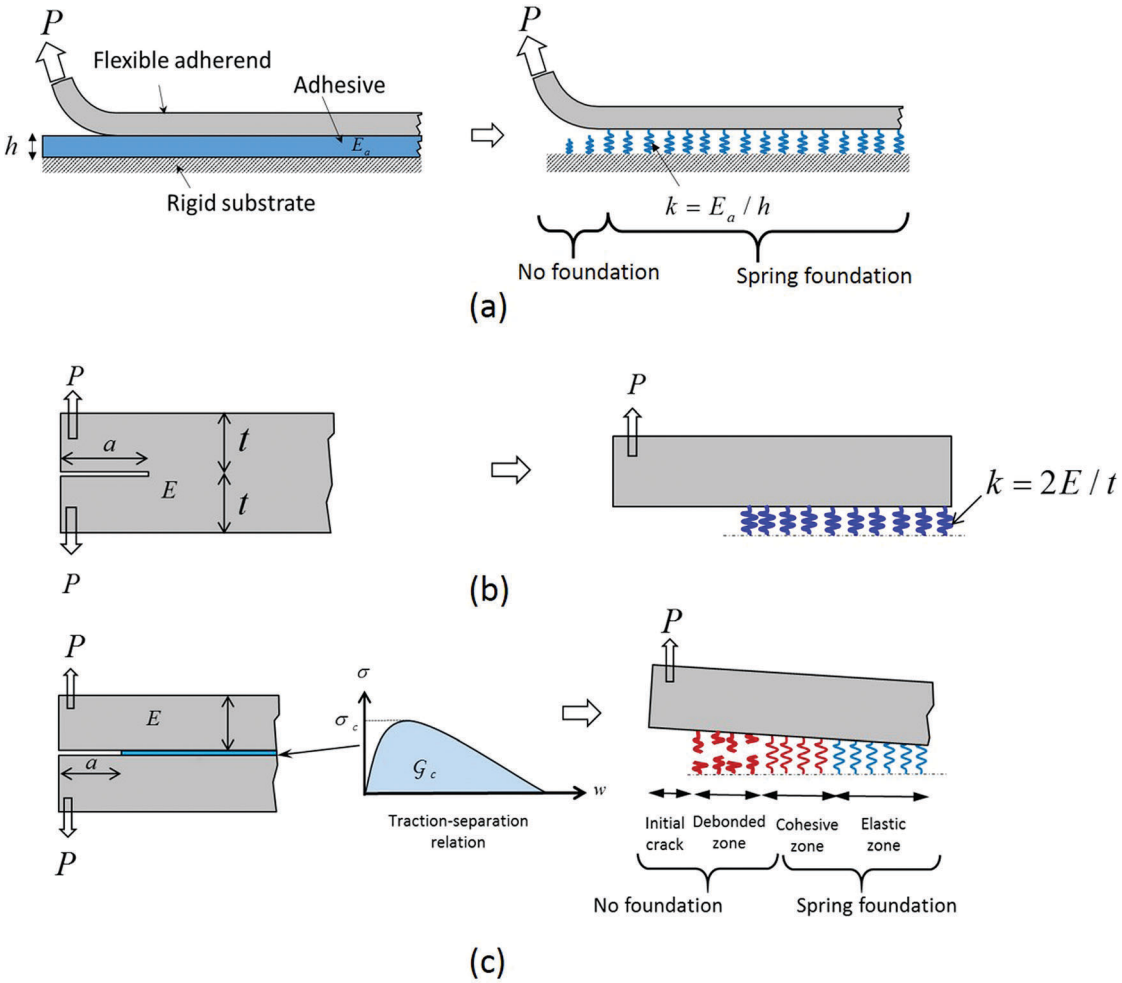

Fig. 2 Schematic sketches of (a) the peeling of a flexible adherend from an adhesive layer bonded to a rigid substrate – a class of problems[16–20] in which the adhesive layer is modelled as a Winkler spring foundation with the spring constant given by the modulus to thickness ratio of the adhesive; (b) the problem analyzed by Kanninen[21] for fracture in monolithic materials, in which the Winkler spring is characterized by the ratio of the modulus to half thickness of one arm of the DCB; and (c) the class of DCB fracture problems in which the adhesive layer is modelled using a traction–separation relation.[25,26]

1958 criterion for debonding,[17] and soon thereafter in Kaelble's[18–20] papers on the stress distributions within pressure sensitive adhesives undergoing peeling. One interesting application to monolithic materials rather than bonded systems was Kanninen's 1973 double cantilever beam (DCB) solution,[21] in which there is no separate layer (*e.g.*, adhesive) upon which to assign a foundation stiffness. Instead, Kanninen modeled the foundation stiffness based on the contributions of the out of plane stiffness of the DCB arms themselves by using half the arm thicknesses to effectively capture the deformation from the centerline back to the neutral axes. This approach serves as a basis for many later contributions in the field of structural adhesives, such as for asymmetric bonded DCB specimens.[22] Krenk[23] modeled the adhesive layer as a Winkler spring foundation using the ratio of its plane stress modulus and the thickness in order to account for the compressibility of a thick adhesive interlayer. Jumel *et al.*[24] used the plane strain foundation modulus to thickness ratio to account for the constraint effects when modeling a thin adhesive layer. Since Stigh's 1988 closed-form solution,[25] Winkler's foundation concept has also been extensively applied to the analyses of the separation/splitting of adherends using the cohesive zone model (CZM) methodology.[26–31] In CZM applications, the foundation spring behavior is characterized by a traction–separation (TS) relation, enabling the quantification of the crack/debond tip process zone (cohesive zone) size as a function of the geometric and the material parameters. For a more detailed review of the application of Winkler foundation analysis in a family of DCB problems, the readers are referred to a recent review article.[32]

We would be remiss in discussing BoEF applications to adhesion without mentioning the important extension to coatings. Lacking the discrete foundation layer evident in adhesive bond applications, stress analysis for coatings considerably softer than the substrate, Kanninen-like assumptions for the coating have been employed to estimate interfacial peel and shear stresses in bonded coatings.[33] Alternatively, for the case

where the coating is much stiffer than the substrate, periodic wrinkling can occur[34,35] under in-plane compression (see Fig. 3) for both bonded elastomeric substrates and for films floating on liquid[36] supporting layers. For such deformations, the foundation spring stiffness stems directly from Biot's analysis[6] for sinusoidal loading of wavelength ξ which gives rise to an effective spring constant of $E_a(2\pi/\xi)$. Huang[37] contributed significantly to this subject of surface wrinkling using a rather rigorous analysis of linear (visco)elasticity to approximate deformations of the foundation.

3. Classical coupling contributions and modifications

The ubiquitous applications of Winkler's BoEF model have been based in part on the simplicity of the model – that the restoring force on the beam or plate is linearly proportional to the deflection at that point only. This simplicity, however, belies the complications that can arise due to several coupling effects. Although Winkler's model is derived and typically expressed for continuous systems, illustrations show the foundation as a series of discrete axial springs, which lends to the idea that each spring acts independently of the other. The Winkler model inherently neglects resistances arising for continuous foundations from both the spatial derivative of the deflection, which imposes shear deformation in the foundation layer (*i.e.*, assumes foundation shear modulus is zero), and the integral of the nearby deflections, through which foundation compressibility enters the solution (*i.e.*, assumes foundation bulk modulus is zero). Kerr provides a formal development of foundation models[38] and also reviews and critiques[39] multiple approaches to include shear coupling to effectively incorporate the shear modulus of a continuous foundation on the behavior, including through the addition of either a fictitious pre-stressed membrane (Filonenko-Borodich foundation)[40] or intermediate beam or plate (Hetényi foundation),[3] along with numerous refinements suggested by several authors and illustrated in Fig. 4. For Pasternak's[41,42] model derived by assuming that the continuous foundation's transverse displacements (perpendicular to the beam/plate on the foundation) and displacement gradients are large as compared to those of the in-plane displacements, Kerr[39] reports the following expression for the restoring traction between the plate and the foundation:

$$q = kw - G\nabla^2 w \tag{5}$$

where G is the shear modulus of a shear-deformable layer mounted atop the spring foundation. The equation governing deformations, for a Kirchhoff–Love plate supported on a Pasternak foundation, derived by Kerr,[39] has the term $\frac{G}{c}\nabla^6 w$, where c is a constant. However, one cannot deduce from it the governing equation for the plate when the foundation material is linearly elastic and incompressible. Kerr also raises the issue of additional boundary conditions needed for the foundation shear for the 6th order GDE that results. The Filonenko-Borodich foundation model, in which Winkler's springs are assumed to be connected with a linearly elastic membrane stretched by a uniform tension T, results in a restoring traction identical to (5), but with T substituted for G. Schiel[43] studied deformations of an Euler–Bernoulli beam supported on a heavy liquid having surface tension σ, and showed that the reaction traction q is given by (5), with k and effective G related to σ.

Variational methods[44,45] do provide a natural means to include foundation effects, including with shear coupling as seen in the potential function given as:

$$\begin{aligned}\Pi = &\frac{D}{2}\iint_{\Omega}\left[(\nabla^2 w)^2 - (1-\nu)\left(\frac{\partial^2 w}{\partial x^2}\frac{\partial^2 w}{\partial y^2} - \left(\frac{\partial^2 w}{\partial x \partial y}\right)^2\right)\right]\mathrm{d}x\mathrm{d}y \\ &- \iint_{\Omega} qw\,\mathrm{d}x\mathrm{d}y - \int_{\Gamma}\left(F_z w + M_s\left(\frac{\partial w}{\partial n}\right)\right)\mathrm{d}s \\ &+ \frac{1}{2}\iint_{\Omega}\int_0^h \left(\sigma_x\varepsilon_x + \sigma_y\varepsilon_y + \sigma_z\varepsilon_z + \tau_{xz}\gamma_{xz} + \tau_{yz}\gamma_{yz} + \tau_{xy}\gamma_{xy}\right)\mathrm{d}z\mathrm{d}x\mathrm{d}y\end{aligned} \tag{6}$$

where Ω is the plate mid-surface, Γ is the perimeter of the mid-surface, F_z is the vertical force distribution around the edge of the plate, M_s is the component of the edge moment parallel to the edge of the plate, and the stress and strain components in the triple integral are within the foundation layer. Here, s and n represent directions parallel to the edge of the plate and normal to that edge, respectively. Minimizing this potential function with trial functions satisfying the displacement-type boundary conditions provides approximate solutions to the problem and permits more general coupling mechanisms to account for the influence of the foundation.

Vlasov and Leont'ev[44] describe several models of a linearly elastic foundation in which both transverse and shear deformations are considered. The top surface of the foundation supports the beam and the bottom surface rests on a rigid stationary flat base.

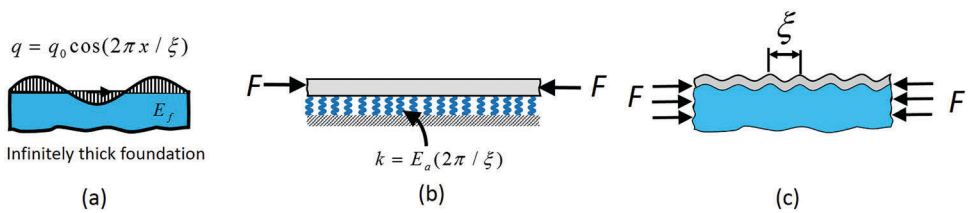

Fig. 3 Schematic illustration of the application of Winkler foundation in analyzing surface wrinkling under in-plane compression: (a) Biot's configuration,[6] (b) equivalent BoEF configuration, and (c) wrinkling phenomenon.

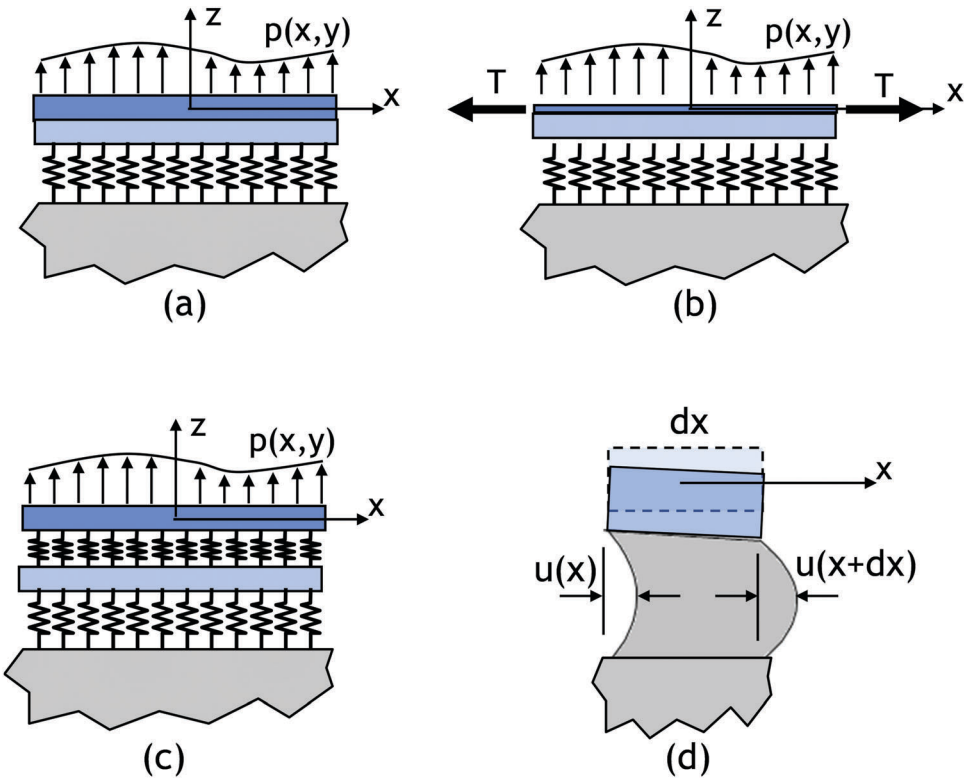

Fig. 4 Illustrations of configurations considered for coupled foundation contributions: (a) through addition of a shear deformable layer sandwiched between plate and foundation, (b) through the use of shear deformable layer between a stretched membrane and the foundation, (c) through the use of a shear deformable layer suspended by elastic foundations above and below, and (d) through considering the incompressibility of an elastomeric layer, showing the increasing bulging of elastomer in a differential element when the plate experiences a downward (negative w) displacement (2-D image only).

By dividing the foundation into several layers, approximating the transverse displacement in each layer by a simple (arbitrary) function of the depth (axial) co-ordinate, and using equilibrium equations of linear elasticity, they recover all of the foundation models described above and deduce expressions of constants appearing in (1), (3) and (4) in terms of Young's modulus and Poisson's ratio of the foundation material. Vlasov and Leont'ev[44] state that the Russian academician Fuss effectively proposed the Winkler hypothesis in 1801. Jones and Xenophontos[45] have provided an alternative variational formulation of the Vlasov's two-parameter model, determined their values in terms of the foundation parameters, and have shown that its predictions agree well with the test results. A recent review of the subject also includes comments on numerical solution approaches.[46]

4. Coupling arising from interlayer incompressibility

For an incompressible, linearly elastic, isotropic material, the bulk modulus equals infinity and the dilatational strain vanishes. Thus equilibrium equations of linear elasticity are modified by introducing and including an indeterminate hydrostatic pressure which is found by solving the equations of equilibrium with normal surface tractions prescribed on a part of the bounding surface of the body. For a linearly elastic foundation made of an incompressible material, *e.g.*, clay, with Young's (or the shear) modulus varying linearly with the depth from the top surface supporting a beam/plate, Lekhnitskii[47] and Gibson[48] have independently deduced Winkler's formula.

In spite of the connection between shear and bulk properties, however, none of the classic models proposed to incorporate foundation shear stiffness appear to have addressed the role of material compressibility for foundations of finite thickness. This is the situation that arises, for example, with adhesive bonds wherein the finite-thickness elastomeric layer can be treated as a foundation. For an elastomeric foundation with the shear modulus much lower than the bulk modulus, the material incompressibility can play a significant role that dominates for highly constrained configurations.

4.1 Development of solution based on lubrication theory

Lefebvre *et al.*[49] hinted at this issue when the measured stiffness of DCB specimens involving steel beams bonded with a neoprene interlayer suggested discrepancies with their BoEF analysis, leading them to speculate on the role that elastomer "incompressibility" might play in the analysis. This finding provided the impetus for Dillard's subsequent analysis[50] in 1989 of a plate supported by a continuous elastomeric foundation. The resulting 6th order GDE built on the 4th order Winkler

solution to include the coupling resulting from the constraint of an incompressible foundation layer, where the restoring force follows the classic Reynolds equation[51] for lubrication theory, as used by Gent and Meinecke[52] for elastomers:

$$\nabla^2 q = -\frac{12\mu w}{h^3} \tag{7}$$

Here the restoring traction q equals the negative of the hydrostatic pressure within the elastomer, μ is the shear modulus of the elastomer and h its thickness, which is assumed to be significantly larger than the deflection, w. This equation results from the equations of motion and the constitutive equation of a linearly elastic and incompressible material upon applying assumptions used in lubrication theory.[52,53] As opposed to a spring foundation, which does not take into account any horizontal displacement, according to lubrication theory the horizontal displacement in an elastomeric foundation varies in a parabolic fashion through the thickness of the elastomer foundation, as illustrated schematically in Fig. 5. The resulting GDE (for general and plane strain or cylindrical bending) and the characteristic reciprocal length are:

$$\begin{aligned} &\text{General}: \ \nabla^6 w - \lambda_e{}^6 w = \frac{1}{D}\nabla^2 p \\ &\text{Cylindrical}: \ \frac{\mathrm{d}^6 w}{\mathrm{d}x^6} - \lambda_e{}^6 w = \frac{1}{D}\frac{\mathrm{d}^2 p}{\mathrm{d}x^2} \\ &\text{Reciprocal length}: \ \lambda_e = \sqrt[6]{\frac{12\mu}{Dh^3}} \end{aligned} \tag{8}$$

The complimentary solution for the cylindrical bending problem is:

$$\begin{aligned} w(x) \ = \ & C_1 \mathrm{e}^{-\lambda_e x} + C_2 \mathrm{e}^{\lambda_e x} + C_3 \mathrm{e}^{-\frac{\lambda_e x}{2}} \cos\frac{\sqrt{3}\lambda_e x}{2} + C_4 \mathrm{e}^{-\frac{\lambda_e x}{2}} \sin\frac{\sqrt{3}\lambda_e x}{2} \\ & + C_5 \mathrm{e}^{\frac{\lambda_e x}{2}} \cos\frac{\sqrt{3}\lambda_e x}{2} + C_6 \mathrm{e}^{\frac{\lambda_e x}{2}} \sin\frac{\sqrt{3}\lambda_e x}{2} \end{aligned} \tag{9}$$

In contrast to the Winkler solution, the arguments for the exponential terms and the sinusoidal terms now differ by a factor of $\sqrt{3}$, meaning that the oscillations decay (from loading point) at a slower rate compared to the oscillation period, resulting in more pronounced undulations. Because of the non-oscillatory terms, the distance between the zero-crossing points is not quite constant, but the characteristic length, $\lambda_e{}^{-1}$, retains a similar physical meaning relating plate stiffness to elastomer stiffness. From the expressions of the reciprocal lengths, λ_w given in (3) and λ_e in (8), it can be shown that $\lambda_w \approx 0.61\alpha^{-1/4}\lambda_e$, where $\alpha = (D/\mu h^3)^{1/3}$. The dimensionless number, α, is commonly regarded as the lateral confinement[54] of the elastomer layer. The lateral confinement of an elastomeric layer may amplify its effective stiffness significantly.

Direct comparison of the Winkler and incompressible elastomer layer solutions are difficult,[55] as differences depend strongly on the confinement, α. Comparisons of the deflections and various derivatives, as well as of the lateral deformation and traction within the elastomeric layer, were given for the plane strain cases of an applied line load and applied line moment on an infinite plate.[50] These cases are among the easiest to compare, as the boundary conditions require that values and derivatives for plate and lateral elastomer displacements vanish at long distances from the point of load or moment application. Results for the former case for $x \geq 0$ are given below (see eqn (10)), when a centrally applied ($x = 0$) line force, $P_e = \frac{72\mu}{h^3\lambda_e{}^3}$ for the elastomer model or $P_w = \frac{2k}{\lambda_w}$ for the Winkler foundation, causes equivalent deflections of $w(0) = \hat{w}$.

$$\begin{aligned} w(x) \ &= \hat{w}\phi_j(x\lambda_j) \\ \theta(x) &= \frac{\mathrm{d}w}{\mathrm{d}x} = \hat{w}\lambda_j\phi_j{}'(x\lambda_j) \\ M(x) &= D\frac{\mathrm{d}^2 w}{\mathrm{d}x^2} = \hat{w}\lambda_j{}^2 D\phi_j{}''(x\lambda_j) \\ V(x) &= D\frac{\mathrm{d}w^3(x)}{\mathrm{d}x^3} = \hat{w}\lambda_j{}^3 D\phi_j{}'''(x\lambda_j) \\ q(x) &= -D\frac{\mathrm{d}w^4}{\mathrm{d}x^4} = -\hat{w}\lambda_j{}^4 D\phi_j{}''''(x\lambda_j) \\ u_e\left(x,\frac{h}{2}\right) &= \frac{h^2}{8\mu}\frac{\mathrm{d}q}{\mathrm{d}x} = -\frac{\hat{w}\lambda_j{}^5 h^2 D}{8\mu}\phi_j{}''''(x\lambda_j) \end{aligned} \tag{10}$$

Here the subscript 'j' stands for either 'e' or 'w', which we have used, respectively, for the elastomeric and the Winkler foundations, and primes denote differentiation with respect to x. The last line represents the horizontal displacement along the midplane of the elastomeric layer ($z = h/2$), and does not apply to the Winkler foundation. Fig. 6 exhibits the plots of ϕ_j and its derivatives (in other words, nondimensionalized versions of the

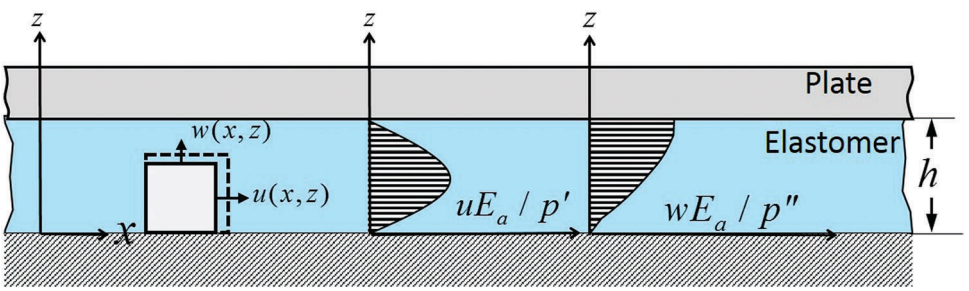

Fig. 5 Schematic illustrating the distributions of vertical and horizontal displacements (nondimensionalized as shown) at a given location in the elastomeric foundation. The horizontal displacement at the top interface is negligible as a consequence of no-slip boundary condition and neglecting in-plane displacements on the plate bounding surfaces. Here prime means derivative with respect to x.

quantities listed in (10)) as functions of $x\lambda_j$ for the two foundations. Only the relative magnitudes and decay rates should be compared, as the axes are normalized by two different quantities for the two foundations because of the fundamental difference in λ_j as well as the magnitudes of forces required to achieve the prescribed displacement, $\hat{w}$. Nevertheless, stark differences are clearly seen for the spatially dependent ϕ_j functions. Behaviors resulting from other boundary conditions are being explored, along with comparing Winkler approximations to the elastomer foundation problem.[55]

Interestingly, a 6th order GDE is obtained for the Reissner foundation[56] and Pasternak's foundation (according to Kerr's paper[39]) as well. These, however, result from a foundation's shear contributions modelled by a fictitious intermediate plate suspended by two layers of spring foundation, so bulk stiffness was still not considered. Bert[57] extended this analysis to the case of foundations of arbitrary Poisson's ratio, noting consistency with Lefebvre *et al.*[58] for $\nu = 1/2$ and with Lai *et al.*[59] for slightly compressible foundations.

The model in (8) neglects the effects of shear stresses at the interface on layer deflections, consistent with ignoring in-plane deflections, as discussed in Section 1. It should also be noted that this approach effectively assumes that the normal traction exerted across the plate-to-interlayer interface is equivalent to negative of the hydrostatic pressure, as appropriate for lubrication theory. An additional term can be added to reflect the superposed uniaxial stress,[52] resulting from $k = E_a/h = 3\mu/h$ for an elastomer:

$$\begin{aligned}
&\text{General}: \ \nabla^6 w + 4\lambda_w{}^4\nabla^2 w - \lambda_e{}^6 w = \frac{1}{D}\nabla^2 p \\
&\text{Cylindrical}: \ \frac{\mathrm{d}^6 w}{\mathrm{d}x^6} + 4\lambda_w{}^4\frac{\mathrm{d}^2 w}{\mathrm{d}x^2} - \lambda_e{}^6 w = \frac{1}{D}\frac{\mathrm{d}^2 p}{\mathrm{d}x^2} \\
&\text{Reciprocal length}: \ \lambda_e = \sqrt[6]{\frac{12\mu}{Dh^3}} \\
&\qquad\qquad \lambda_w = \sqrt[4]{\frac{3\mu}{4Dh}} = \sqrt[4]{\frac{E_a}{4Dh}}
\end{aligned} \tag{11}$$

This model should effectively bridge between low and high constraint scenarios, where Winkler and lubrication theory models are respectively applicable. The authors are not aware of this revised form having been reported in the literature. Allowing for the possibility that D, h, and even μ could be functions of x and y, the general form can also be written as:

$$12\mu w = \nabla\cdot\left[h^3\nabla\left(D\nabla^4 w + \frac{3\mu}{h}w - p\right)\right] \tag{12}$$

This is equivalent to combination of the lubrication and buoyant plate solutions (discussed in Section 5) from the analogous response of a viscous fluid foundation, with the caveat that once the elastomer is crosslinked (physically or chemically) at a given thickness, h, which can vary spatially in the initial fabrication, becomes a reference configuration. Thus nonlinear effects are expected to arise unless $w \ll h$, a limitation that does not exist for the analogous fluid foundation.

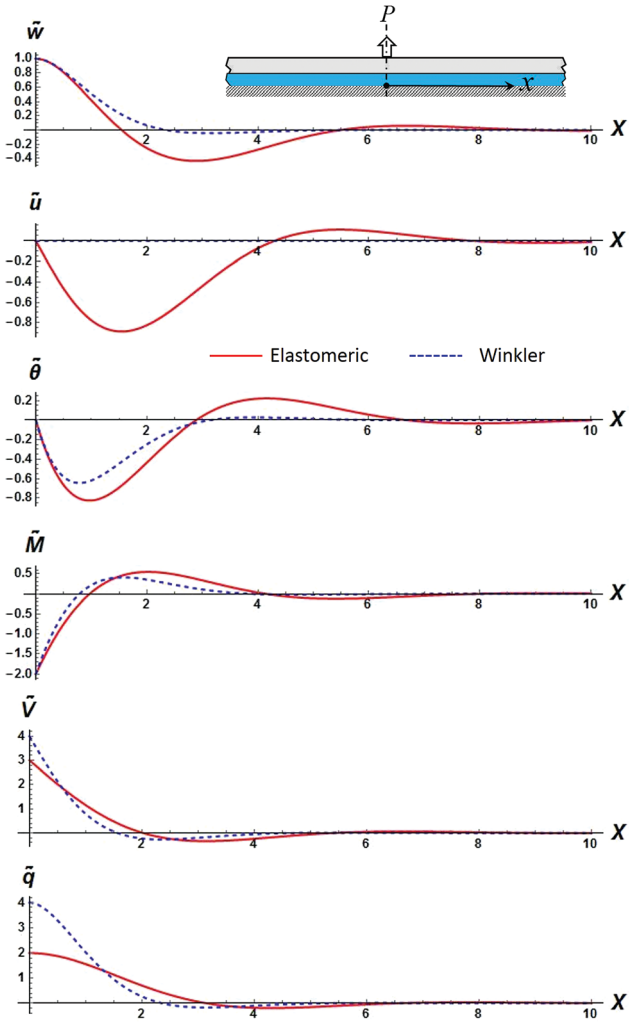

Fig. 6 Comparisons of nondimensionalized plate deflection ($\tilde{w}$), the lateral displacement ($\tilde{u}$) of the mid-plane of the foundation, the slope of the plate ($\tilde{\theta}$), the bending moment ($\tilde{M}$), the shear force ($\tilde{V}$), and the restoring traction ($\tilde{q}$) provided by the foundation as functions of the horizontal nondimensionalized distance X from the load application location ($X = 0$). Here $\tilde{w} = w/\hat{w}$, $\tilde{u} = u\Big/\left(\frac{\hat{w}D\lambda_j{}^5h^2}{8\mu}\right)$, $\tilde{\theta} = \theta/(\lambda_j\hat{w})$, $\tilde{M} = M/(\hat{w}D\lambda_j{}^2)$, $\tilde{V} = V/(\hat{w}D\lambda_j{}^3)$, $\tilde{q} = q/(\hat{w}D\lambda_j{}^4)$ and $X = x\lambda_j$. The inset is a schematic of the problem for which the results are plotted.

4.2 Debonding of a plate from an elastomeric foundation

A problem which becomes particularly relevant in soft matter adhesion is that of debond propagation under the action of peel stress. When a plate is peeled from an elastomeric layer by application of transverse load at its overhanging edge, debonding begins to propagate as soon as the interface is stressed beyond capacity. However, when the confinement parameter becomes sufficiently large, the onset of interfacial fingering instabilities is observed at the advancing debond front.[60] Although their initial studies of meniscus instabilities used the Winkler foundation[62] concept for establishing scaling arguments for the finger lengths, Ghatak and Chaudhury independently recognized the issues arising from elastomer foundation incompressibility.[54] They subsequently presented their pioneering

work on soft matter fingering and instabilities in a series of papers[54,61–64] in the context of displacement-controlled peeling of a flexible plate from a thin elastomeric layer bonded to a rigid base as shown schematically in Fig. 7a. While the details of interfacial stresses near the interface edge/corner[65,66] cannot be resolved using the approximate analysis based on lubrication theory, the assumption of vanishing peel stress at the tip of an interfacial crack[64] leads to a peak in the peel stress occurring at a distance of $\sim\lambda_e^{-1}$ from the edge. This could explain the experimental observations of internal debonding and the associated adhesion-induced instability (Fig. 7c) resulting ultimately in the propagation of a convoluted crack front exhibited in Fig. 7d. Drawing inspiration from the remarkable adhesive properties of patterned insect toe-pads, they argued that an adhesive foundation could be micro-structured at a length scale smaller that the length $\sim\lambda_e^{-1}$ to engineer cavity nucleation and a concomitant increase in the effective adhesion reflected in the stick-slip behavior in the experimentally obtained moment–displacement curves. Their findings were further supported by experimental observations of Chung and Chaudhury.[67] In a subsequent study,[63] the elastomer foundation analysis was used in developing a test method to measure the work of adhesion for an elastomer/plate interface using the similar peeling experiment but without patterns being present at the interface. Disregarding the complex crack initiation mechanism and assuming a straight crack front for simplicity, the peel stress was set to be maximum at the edge/corner. They derived for the strain energy release rate $G_c = 9D\Delta^2 g(a)/2a^4$ where the function $g(a)$ resulted from the solution of (8). Ghatak[68] extended his analysis of peeling later to explain earlier experimental findings of adhesion-induced instability manifested in the form of a fingerlike crack front,[54] proving that adding a sinusoidal perturbation to the base solution obtained using a straight crack front (plane-strain cylindrical bending problem) resulted in a lower energy configuration when the elastomer confinement is sufficiently large. Building on this work, Mukherjee *et al.*[60,65] investigated debonding of soft matter layers between rigid and flexible adherends (Fig. 7b) using the CZM, schematically illustrated in Fig. 8a along with resulting peel stress distribution. It is worth mentioning that neither of the mechanics of materials solutions[63,64] of the peeling problem captures the singular stress field[65,66] near the interface edge/corner. Also of note is that energetically-favored debonding (involving discrete or fingering debond patterns), cavitation, or other void-inducing damage can significantly relieve the volumetric constraint that necessitates the 6th order GDE, allowing Winkler's spring foundation behavior to effectively be applicable in these regions. A recent example incorporating a bilinear traction–separation relation resulted in a 4th order term in the cohesive zone in addition to the 6th order term which dominantly governed the behavior of the region over which the elastomer remained intact.[65] For cases such as the behavior of pressure sensitive adhesives, which undergo extensive cavitation and fibrillation within the debond damage zone, the fibrils may represent independent springs, as assumed in Winkler's solution, though may reorient substantially, complicating CZM representations.[69] Recent papers have addressed buckling of plates on elastomeric layers of finite thickness under uniaxial[70] and biaxial[71] compression.

The effect of compressibility of the foundation has been recently captured well by an extended Winkler foundation

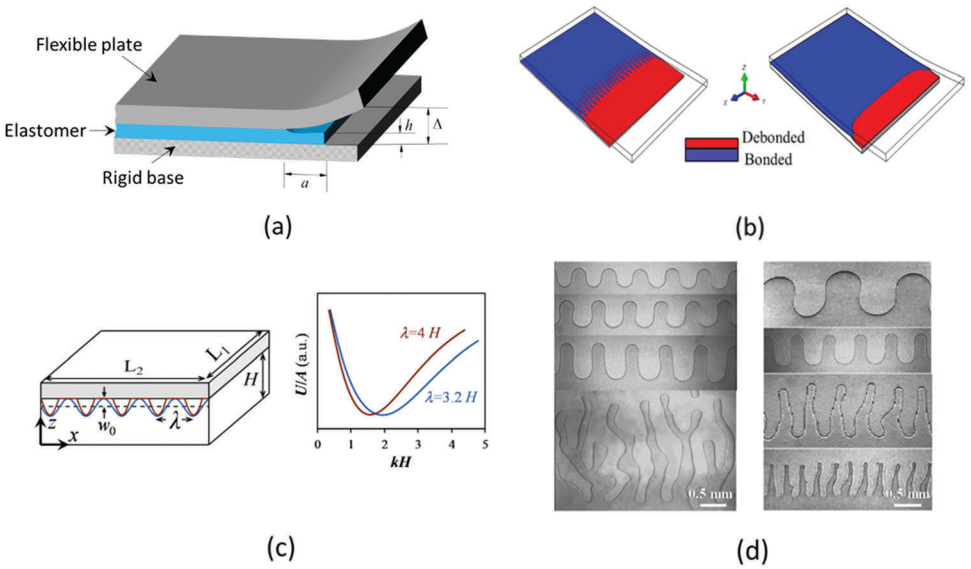

Fig. 7 Images summarizing works on peeling from a soft elastomeric adhesive layer: (a) a schematic sketch of the experimental configuration for displacement-controlled peeling of a flexible plate from an elastomeric layer bonded perfectly to a rigid base; (b) snapshots from FE simulation of the problem conducted using a TS relation to model the interfacial interaction. (c) (left) Schematic of a model to evaluate the fingering wavelength (or wavelength of instability) on peeling of a rigid contactor from a thin elastic layer bonded to a rigid substrate. (right) Plot of excess energy associated with the appearance of the instability for single mode perturbation (blue curve) and half rectified sine wave deformation profile (maroon curve). (d) Fingering patterns emerging in the contact line on removing a thin flexible plate from a thin PDMS sample. Image (b) is reprinted from ref. 60 with permission from Elsevier. Images (c) and (d) are reprinted from ref. 61 with permission from Springer Nature.

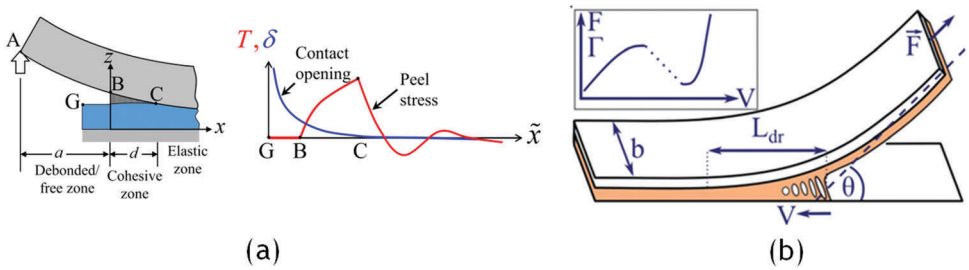

Fig. 8 Deviation from linear models suggested above when damage occurs: (a) sketch of edge debonding in peeling of a thin flexible plate from an elastomer layer, along with various zones near the debonding tip B after the debond has moved the corresponding contact opening (displacement jump) profile along the x-axis; and in (b) illustrating peeling of a viscoelastic pressure sensitive adhesive with typical variations of the peeling force F and of the adhesion energy Γ with the peeling velocity V. L_{dr} is the characteristic extension of the debonding region, where the adhesive is significantly strained. Image (a) is reproduced from ref. 65 with permission from ASME. Image (b) is reproduced from ref. 72 with permission from The Royal Society of Chemistry.

analysis conducted by Cabello *et al.*[73] They proposed for the DCB class of problems, a spatially varying Winkler spring stiffness for the adhesive interlayer, effectively capturing the transition of the stress state from tri-axial over the inner portion of the bondline to a plane stress state prevailing near the free edges of the adhesive layer. Their approximate model, albeit based on an empirical relation found using an experimental/numerical approach, predicted for two example cases the internal peak of peel stress that is expected to occur for confined elastomeric interlayers.

5. Analogous fluid foundations

Winkler's foundation has been used to obtain a mathematical formulation for the displacement of elastic plates submerged in a liquid or in contact with a liquid as early as Hertz's analysis in 1884.[74] Bikerman and Yap[75] highlighted the coupling between the fluid viscosity and the flexural rigidity of a plate during the peeling from a Newtonian fluid, while Piau *et al.*[76] incorporated the lubrication effects of the adhesive during steady-state peeling. More recently, there has been an increased interest to study detachment from a fluid foundation. This scenario is encountered in animal locomotion,[77,78] printing,[79] blister formation,[80] and adhesion[54,72,76,81–83] (see Fig. 9). For example, transfer printing is used to facilitate the addition of semiconductor inks on a substrate of interest for the fabrication of microelectronic or optoelectronic elements.[84–86] The stamp for transfer printing is made of a membrane that contacts the ink and later releases it through a pressure difference. As the stamp is slowly retracted, the membrane peels out of contact with the ink. The variation of pressure causes deflection of the membrane and can be modelled as a plate on a fluid foundation, when bending stiffness dominates. Moreover, the Winkler foundation can also be used to analyze vibration and structural instability of carbon nanotubes conveying a fluid[87] (Fig. 9b). Interestingly, many elastic foundation models in contact with a fluid and exposed to vibration prefer to use Pasternak equation[88] because of its simplicity amongst two parameter models which can better describe the displacements on the boundary of uniformly loaded surface area.

A large number of animals can climb on smooth surfaces using adhesive pads, the surface area of which has been found to depend on the mass of these animals.[89] In particular, the locomotion of tree frogs on wet or submerged surfaces involves a peeling motion analogous to the one illustrated in Fig. 9a. Insects have also been shown to secrete adhesive fluids that aid in their attachment to smooth surfaces.[90] These wet biological adhesives have also been shown to have a rate-dependent adhesion.[91] In general the presence of a viscous fluid foundation brings a purely dissipative, time-dependent aspect, to adhesion. Moreover, the wide range of adhesion properties observed with different species of tree frogs correlates strongly with the compliance of their toe pads,[92] which is analogous to dry adhesion observations as well.[93–97] As a result, understanding the coupling between elastic compliance and viscous forces during peeling in fluid environments is necessary to comprehend wet adhesion. Unsteady dynamic peeling from an elastomeric foundation, as studied by Ghatak and Chaudhury,[54] was later extended to the case of wet biomimetic adhesives on structured surfaces[63] that highlighted the contribution of viscous losses to adhesion.

The case of a growing fluid blister is particularly analogous to the case of elastic foundations (Fig. 9c). The formation of a blister in a fluid-mediated radial elastic peeling can occur over a broad range of length scales: from the manufacture of flexible electronics and microelectromechanical systems (MEMS)[100] to the geological formation of laccoliths formed by the flow of viscous magma beneath an elastic sediment layer.[101] Delaminations of an axially compressed sheet from a fluid interlayer, analogous to fracture or debonding with solid interlayers, are also possible.[102] During the formation of a blister (see Fig. 9c) a viscous fluid is pumped beneath an elastic sheet. The propagation of the viscous fluid depends on the dynamics at the peeling front of the elastic sheet and affects the shape of the blister.[103] In this scenario, the rate of change in deflection of the elastic sheet depends on the coupled effects of viscous forces of the fluid and the bending and tension of the elastic sheet,[80,101] leading to:

$$12\eta\frac{\partial w}{\partial t} = \nabla\cdot\left[w^3\nabla\left(D\nabla^4 w + \rho_f g w - p\right)\right] \qquad (13)$$

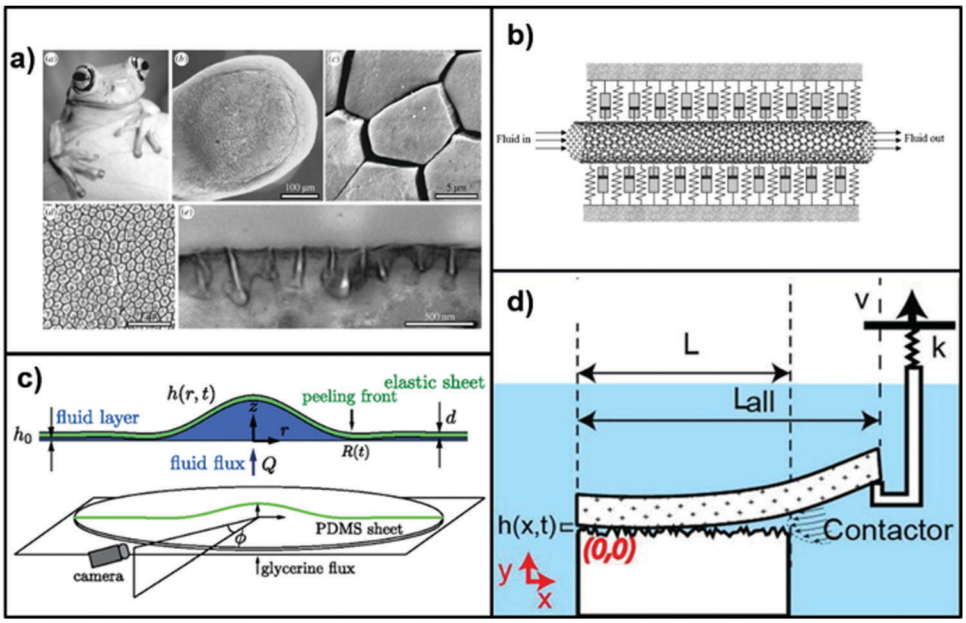

Fig. 9 Applicability of Winkler's analysis for fluid foundations. (a) Morphology of tree frog toe pads showing a microstructure that consists of an epidermis with hexagonal epithelial cells. Secretion of fluid can mediate adhesion between tree frog toe pad and the contacting surface. Moreover, infusion of external fluid may also occur during detachment of tree frog toe pad in a fluid medium. Adhesion can also be affected by fluid trapped within gaps between hexagonal structures or between the toe pad and contacting surface. (b) Schematic of a carbon nanotube conveying fluid on a viscoelastic Winkler foundation for applications of CNTs as nanocontainers, nanopipes and nanothermometers. (c) Schematic of the formation of a fluid blister caused by an influx of fluid generating a radial peeling front. (d) Schematic of peeling experiment where contact and detachment happen in fully submerged conditions. During peeling, a rigid contactor lifts one end of the top plate, causing detachment with a small (<5°) peel angle. Image (a) is reproduced from ref. 98 with permission of The Royal Society. Image (b) is reprinted from ref. 87 with permission of Elsevier. Image (c) is reprinted with permission from ref. 80 © (2013) by the American Physical Society. Image (d) is reprinted from ref. 99 with permission of AIP Publishing.

where η is the fluid viscosity, and w is the deflection of the plate as before. However, the deflection is taken to be zero when this plate is in contact with the substrate, so is a direct measure of the thickness of the fluid layer. This is very similar to (12), but without the limitation requiring limited thickness variations, as was the case for a crosslinked elastomer. The 6th order GDE (13) again arises from the mass conservation applied to the incompressible fluid within the lubrication theory approximation (*i.e.*, the deflection of plate is much smaller than the lateral dimensions). The relationship between the fluid flow rate and its hydrostatic pressure gives rise to a fourth derivative of the deflection of the elastic plate. Additionally, the interfacial crack initiated by the pumping of a finite volume of liquid can equilibrate at a set blister radius and height. Adhesion energy of thin films can be evaluated using such experiments as shown in a recent study.[104]

Investigations of the coupling between lubrication forces, compliance, and surface topography have also been performed for unsteady peeling in fluids of different viscosity.[99,105] Here two small plates are separated by a fluid film and the distributed pressure causing the adhesive force is the lubrication force over the nominal length of the plate being peeled (see Fig. 9d). The flexural rigidity, the transverse (out-of-plane) extensional compliance of the plate, and the fluid viscosity all increase the maximum debonding force and energy release rate. There is a competition between the relative importance of the flexural rigidity of the plate and the viscosity of fluid on the detachment force. For insects adhering to surfaces in low viscosity fluids like water, the flexural rigidity of their toe pads would be expected to play a more important role in adhesion rather than the dissipative viscous forces caused by fluid infusion. In addition to flexural rigidity, the extensional compliance of the elastic plate can also compete with viscous forces.[99]

6. Compilation of models

Table 1 summarizes the range of plate solutions that have been proposed and used, building on the original Winkler foundation. As mechanics of materials level solutions, all involve certain assumptions, including quasi-static loading conditions and the requirements of Kirchhoff–Love plate theory that normals remain straight and normal to the mid-surface, linearly elastic (or viscous for hydrodynamic) behavior, and that strains, displacements ($w < t$), and displacement gradients ($|\nabla w| \ll 1$) are all small. In addition, requirements for validity (explicitly given in Table 2, along with their justification) have been added, though explicit magnitudes for the inequalities are not given, and would likely require computational resolution and could be complicated by coupling effects. As an example, however, Goland and Reissner[11] require that $\frac{E_a}{h} \ll \frac{E}{t_p}$ to ensure that the plate thickness changes are negligible, then suggest

Table 1 Summary of the general plate on the Winkler foundation and various extensions

Formulation source	Restoring force	Characteristic reciprocal length	Governing differential equation	Notes and assumptions
Föppl (1922)[10] based on Winkler (1867)[1]	$q = kw$	$\lambda_w = \sqrt[4]{\frac{k}{4D}}$	$\nabla^4 w + 4\lambda_w{}^4 w = \frac{p}{D}$	Original formulation for beam on elastic foundation extended to plates; assumes independent spring support; [1], [2], [3], [4]
Hertz (1894)[74]	$q = \rho_f g w$	$\lambda_w = \sqrt[4]{\frac{\rho_f g}{4D}}$	$\nabla^4 w + 4\lambda_w{}^4 w = \frac{p}{D}$	Solution for a plate floating on a fluid (sufficiently thick to avoid hydrodynamic effects); [2], [4], [5]
Filonenko-Borodich (1940)[40]	$q = kw - T\nabla^2 w$	$\lambda_w = \sqrt[4]{\frac{k}{4D}}$	$\nabla^4 w - T\nabla^2 w + 4\lambda_w{}^4 w = \frac{p}{D}$	Assumes uniform equal biaxial tension of T[1], [2], [3], [4]
Hetényi (1946)[3]	$q = kw + S\nabla^4 w$	$\lambda_w = \sqrt[4]{\frac{k}{4D}}$	$(D + S)\nabla^4 w + 4D\lambda_w{}^4 w = p$	S represents plate rigidity of a fictitious coupling layer [1], [2], [3], [4]
Pasternak (1954)[42]	$q = kw - G\nabla^2 w$	$\lambda_w = \sqrt[4]{\frac{k}{4D}}$	$\nabla^4 w - G\nabla^2 w + 4\lambda_w{}^4 w = \frac{p}{D}$	G is the shear modulus of a ‘‘shear layer’ element’’ [1], [2], [3], [4]
Dillard (1989)[50]	$\nabla^2 q = -\frac{12\mu w}{h^3}$	$\lambda_e = \sqrt[6]{\frac{12\mu}{Dh^3}}$	$\nabla^6 w - \lambda_e{}^6 w = \frac{1}{D}\nabla^2 p$	Uniform plate on (incompressible) elastomeric foundation; assumes hydrostatic stresses within the elastomer layer; [2], [6], [7], [8], [9], [10]
Michaut (2011)[101]	$\nabla^2 q = \rho_f g \nabla^2 w - \frac{12\eta}{w^3}\frac{\partial w}{\partial t}$	$\lambda_w = \sqrt[4]{\frac{3\eta}{4Dw}}$ $\lambda_e = \sqrt[6]{\frac{12\eta}{Dw^3}}$	$12\eta\frac{\partial w}{\partial t} = \nabla\cdot\left[w^3\nabla\left(D\nabla^4 w + \rho_f g w - p\right)\right]$	Includes buoyant and hydrodynamic effects; allows for spatially varying plate stiffness and fluid thickness; w represents (incompressible) fluid layer thickness; [2], [5], [8], [9], [10], [11]
Present work	$\nabla^2 q = \frac{3\mu}{h}\nabla^2 w - \frac{12\mu w}{h^3}$	$\lambda_w = \sqrt[4]{\frac{3\mu}{4Dh}}$ $\lambda_e = \sqrt[6]{\frac{12\mu}{Dh^3}}$	$12\mu w = \nabla\cdot\left[h^3\nabla\left(D\nabla^4 w + \frac{3\mu}{h}w - p\right)\right]$	Relaxes [9], effectively allowing vertical stress difference within incompressible elastomer layer and spatially varying plate stiffness and foundation thickness; [2], [6], [7], [8], [10]

Table 2 List of assumptions and requirements for validity, along with their justification

#	Relationship	Justification
[1]	$k \ll \frac{E}{t_p}$	Stiffness of foundation is much less than out of plane stiffness of plate (to change in thickness)
[2]	$t_p \ll \frac{1}{\lambda_w}$	Plate thickness is small compared to characteristic length; needed to assure a normal remains straight and normal
[3]	$\nu = 0$	Poisson’s ratio of foundation is negligible; eliminates dependence on integral of neighboring deflections
[4]	$\mu = 0$	Shear modulus of foundation is negligible; eliminates dependence on derivative of neighboring deflection
[5]	$\rho_f g \ll \frac{E}{t_p}$	Same as [1]
[6]	$\frac{\mu\alpha}{h} \sim \frac{\mu}{h^3\lambda_e{}^2} \ll \frac{E}{t_p}$	Stiffness of foundation is much less than out of plane stiffness of plate (to change in thickness)
[7]	$\lvert w\rvert \ll h,\ \left\lvert\frac{dw}{dx}\right\rvert \ll 1$	Required for elastomeric solid to satisfy small strains, but (interestingly) not for hydrodynamic condition
[8]	$t_p \ll \frac{1}{\lambda_e}$	Plate thickness is small compared to characteristic length; needed to assure a normal remains straight and normal to mid-surface
[9]	$h \ll \frac{1}{\lambda_e}$	Required to maintain that hydrostatic component of foundation stress is dominant
[10]	$\frac{\mu}{h^2\lambda_e{}^2} \ll K$	Ensures volumetric strains in foundation are negligible compared to displaced volume (K is bulk modulus of foundation)
[11]	$\frac{\eta}{w^4\lambda_e{}^2}\left\lvert\frac{\partial w}{\partial t}\right\rvert \ll \frac{E}{t_p}$	Same as [6]; derivable from Stefan’s adhesion

that $10\frac{E_a}{h} < \frac{E}{t_p}$ is appropriate for single lap joint (with flexible adhesive) analysis. Using finite element analysis, Adams and Peppiatt[106] suggest this can be relaxed to $3\frac{E_a}{h} < \frac{E}{t_p}$ without significantly reducing accuracy.

7. Conclusions

This review is meant as a tribute to Emil Winkler and a recognition of the significance of his 1867 beam on elastic foundation (BoEF) formulation for the field of mechanics in general and adhesion science in particular. Numerous

applications are discussed, providing some historical perspective for the classic Winkler analysis relevant to flat and tubular single lap joints, adherends with curvature mismatch, and fracture analysis of monolithic and adhesively bonded joints. These classical applications to adhesive bonds have typically neglected coupling effects within the foundation layer used to model the adhesive, effectively treating foundation displacements as being independent of nearby deflections. Although there is a rich body of literature addressing a wide range of shear and other coupling behavior, the unique constraint imposed by elastomer incompressibility lends itself to an analysis based on lubrication theory, resulting in a 6th order governing differential equation rather than the traditional 4th order Winkler model. This approach has been widely used in modeling a host of soft matter adhesion issues. The same formulation is applicable not only to elastomeric materials with elastic response, but also to fluids with viscous behavior, opening up further applications to wet adhesion with liquid interfaces. Indeed, the simple mechanics of materials solution provided by Winkler, along with its numerous extensions, has clearly made a profound impact on the mechanics of adhesion and soft matter debonding.

Conflicts of interest

There are no conflicts to declare.

References

1 E. Winkler, *Die Lehre von der Elasticitaet und Festigkeit mit besondere Ruecksicht auf ihre Anwendung in der Technik, fuer polytechnische Schuhlen, Bauakademien, Ingenieure, Maschienenbauer, Architecten, etc.*, H. Dominicus, Prague, 1867.
2 L. Frýba, *Vehicle Syst. Dyn.*, 1995, **24**, 7–12.
3 M. Hetényi, *Beams on elastic foundation: theory with applications in the fields of civil and mechanical engineering*, University of Michigan Press, Ann Arbor, 1946.
4 O. Volkersen, *Luftfahrtforschung*, 1938, **15**, 41–47.
5 F. B. Seely and J. O. Smith, *Advanced Mechanics of Materials*, John Wiley & Sons, Inc., New York, 2nd edn, 1952.
6 M. A. Biot, *J. Appl. Mech.*, 1937, **4**, A1–A7.
7 S. P. Timoshenko and S. Woinowsky-Krieger, *Theory of Plates and Shells*, McGraw-Hill, New York, 1959.
8 H. Hertz, *Wiedemann's Ann. Phys. u. Chem.*, 1894, **22**, 449.
9 H. Hertz and P. H. Lenard, *Schriften Vermischten Inhalts*, 1895.
10 A. Föppl, *Vorlesungen über technische Mechanik*, Druck and Verlag von B. G. Teubner, 5th edn, 1922, pp. 103–108.
11 M. Goland and E. Reissner, *J. Appl. Mech.*, 1944, **11**, A17–A27.
12 J. L. Lubkin and E. Reissner, *J. Appl. Mech.*, 1956, **78**, 1213–1221.
13 D. A. Dillard, *J. Adhes.*, 1988, **26**, 59–69.
14 T. A. Corson, Y. H. Lai and D. A. Dillard, *J. Adhes.*, 1990, **33**, 107–122.
15 C. L. Randow and D. A. Dillard, *J. Adhes. Sci. Technol.*, 2006, **20**, 1595–1613.
16 G. J. Spies, *Aircr. Eng.*, 1953, **25**, 64–70.
17 J. J. Bikerman, *J. Appl. Phys.*, 1957, **28**, 1484–1485.
18 D. Kaelble, *Trans. Soc. Rheol.*, 1959, **3**, 161–180.
19 D. Kaelble, *Trans. Soc. Rheol.*, 1960, **4**, 45–73.
20 D. Kaelble, *Trans. Soc. Rheol.*, 1965, **9**, 135–163.
21 M. F. Kanninen, *Int. J. Fract.*, 1973, **9**, 83–92.
22 F. Xiao, C. Y. Hui and E. J. Kramer, *J. Mater. Sci.*, 1993, **28**, 5620–5629.
23 S. Krenk, *Eng. Fract. Mech.*, 1992, **43**, 549–559.
24 J. Jumel, M. K. Budzik and M. E. Shanahan, *Eng. Fract. Mech.*, 2011, **78**, 3253–3269.
25 U. Stigh, *Int. J. Fract.*, 1988, **37**, R13–R18.
26 J. Williams and H. Hadavinia, *J. Mech. Phys. Solids*, 2002, **50**, 809–825.
27 Z. Ouyang and G. Li, *J. Appl. Mech.*, 2009, **76**, 051003.
28 R. H. Plaut and J. L. Ritchie, *J. Adhes.*, 2004, **80**, 313–331.
29 M. Budzik, J. Jumel, K. Imielinska and M. E. R. Shanahan, *J. Adhes. Sci. Technol.*, 2011, **25**, 131–149.
30 S. Jain, S. R. Na, K. M. Liechti and R. T. Bonnecaze, *Int. J. Fract.*, 2016, 1–9.
31 S. Gowrishankar, H. Mei, K. M. Liechti and R. Huang, *Int. J. Fract.*, 2012, **177**, 109–128.
32 A. Abbaszadeh Bidokhti, A. R. Shahani and M. R. Amini Fasakhodi, *Proc. Inst. Mech. Eng., Part C*, 2017, **231**, 2835–2847.
33 E. Suhir, *J. Appl. Mech.*, 1989, **56**, 595–600.
34 J. Y. Chung, A. J. Nolte and C. M. Stafford, *Adv. Mater.*, 2011, **23**, 349–368.
35 H. G. Allen, *Analysis and Design of Structural Sandwich Panels*, Pergamom Press, New York, NY, 2013.
36 J. Huang, B. Davidovitch, C. D. Santangelo, T. P. Russell and N. Menon, *Phys. Rev. Lett.*, 2010, **105**, 038302.
37 R. Huang, *J. Mech. Phys. Solids*, 2005, **53**, 63–89.
38 A. D. Kerr, *Ing.-Arch.*, 1984, **54**, 455–464.
39 A. D. Kerr, *J. Appl. Mech.*, 1964, **31**, 491–498.
40 M. M. Filonenko-Borodich, *Uchenyie Zapiski Moskovskogo Gosudarstvennogo Universiteta Mekhanica*, 1940, pp. 3–18.
41 P. L. Pasternak, *Nauchno-Isledovatel'skaya Konferencia MISI*, 1937.
42 P. L. Pasternak, *Gosudarstvenrwe Izdatelslvo Literaturi po Stroitclstvu i Arkhitekture*, 1954.
43 F. Schiel, *Zeitsehrift fur angewandte Mathematik utul Mechanik*, 1942, **22**, 255–262.
44 V. Z. Vlasov and U. N. Leont'ev, *Beams, Plates and Shells on Elastic Foundations*, Israel Program for Scientific Translation, Jerusalem, 1966.
45 R. Jones and J. Xenophontos, *Int. J. Mech. Sci.*, 1977, **19**, 317–323.
46 Y. H. Wang, L. G. Tham and Y. K. Cheung, *Progress in Structural Engineering and Materials*, 2005, **7**, 174–182.
47 S. G. Lekhnitskii, *J. Appl. Math. Mech.*, 1962, **26**, 1026–1039.
48 R. E. Gibson, *Geotechnique*, 1967, **17**, 58–67.

49 D. R. Lefebvre, D. A. Dillard and H. F. Brinson, *Exp. Mech.*, 1988, **28**, 38–44.
50 D. A. Dillard, *J. Appl. Mech.*, 1989, **56**, 382–386.
51 O. Reynolds, *Proc. R. Soc. London*, 1886, **40**, 191–203.
52 A. N. Gent and E. A. Meinecke, *Polym. Eng. Sci.*, 1970, **10**, 48–53.
53 A. N. Gent and P. B. Lindley, *Proc. – Inst. Mech. Eng.*, 1959, **173**, 111–122.
54 A. Ghatak and M. K. Chaudhury, *Langmuir*, 2003, **19**, 2621–2631.
55 B. Mukherjee, in preparation.
56 E. Reissner, *J. Appl. Mech.*, 1958, **25**, 144–145.
57 C. Bert, *J. Appl. Mech.*, 1994, **61**, 497–499.
58 D. R. Lefebvre, D. A. Dillard and H. F. Brinson, *J. Adhes.*, 1989, **27**, 19–40.
59 Y. H. Lai, D. A. Dillard and J. S. Thornton, *J. Appl. Mech.*, 1992, **59**, 902–908.
60 B. Mukherjee, D. A. Dillard, R. B. Moore and R. C. Batra, *Int. J. Adhes. Adhes.*, 2016, **66**, 114–127.
61 M. K. Chaudhury, A. Chakrabarti and A. Ghatak, *Eur. Phys. J. E: Soft Matter Biol. Phys.*, 2015, **38**, 82.
62 A. Ghatak, M. K. Chaudhury, V. Shenoy and A. Sharma, *Phys. Rev. Lett.*, 2000, **85**, 4329–4332.
63 A. Ghatak, L. Mahadevan and M. K. Chaudhury, *Langmuir*, 2005, **21**, 1277–1281.
64 A. Ghatak, L. Mahadevan, J. Y. Chung, M. K. Chaudhury and V. Shenoy, *Proc. R. Soc. A*, 2004, **460**, 2725–2735.
65 B. Mukherjee, R. C. Batra and D. A. Dillard, *Int. J. Solids Struct.*, 2017, **110**, 385–403.
66 M. A. Bedia and L. Mahadevan, *Proc. R. Soc. London, Ser. A*, 2006, **462**, 3233–3251.
67 J. Y. Chung and M. K. Chaudhury, *J. R. Soc., Interface*, 2005, **2**, 55–61.
68 A. Ghatak, *Phys. Rev. E: Stat., Nonlinear, Soft Matter Phys.*, 2006, **73**, 041601.
69 R. Villey, P. P. Cortet, C. Creton and M. Ciccotti, *Int. J. Fract.*, 2017, **204**, 175–190.
70 B. Mukherjee and D. A. Dillard, *Int. J. Mech. Sci.*, 2017, DOI: 10.1016/j.ijmecsci.2017.10.015.
71 B. Li, S. Q. Huang and X. Q. Feng, *Arch. Appl. Mech.*, 2010, **80**, 175.
72 R. Villey, C. Creton, P. P. Cortet, M.-J. Dalbe, T. Jet, B. Saintyves, S. Santucci, L. Vanel, D. J. Yarusso and M. Ciccotti, *Soft Matter*, 2015, **11**, 3480–3491.
73 M. Cabello, J. Zurbitu, J. Renart, A. Turon and F. Martínez, *Int. J. Solids Struct.*, 2016, **94**, 21–34.
74 H. Hertz, *Ann. Phys.*, 1884, **258**, 449–455.
75 J. Bikerman and W. Yap, *Trans. Soc. Rheol.*, 1958, **2**, 9–21.
76 J. M. Piau, G. Ravilly and C. Verdier, *J. Polym. Sci., Part B: Polym. Phys.*, 2005, **43**, 145–157.
77 G. Hanna, W. Jon and W. J. Barnes, *J. Exp. Biol.*, 1991, **155**, 103–125.
78 Y. Tian, N. Pesika, H. Zeng, K. Rosenberg, B. Zhao, P. McGuiggan, K. Autumn and J. Israelachvili, *Proc. Natl. Acad. Sci. U. S. A.*, 2006, **103**, 19320–19325.
79 A. Carlson, S. Wang, P. Elvikis, P. M. Ferreira, Y. Huang and J. A. Rogers, *Adv. Funct. Mater.*, 2012, **22**, 4476–4484.
80 J. R. Lister, G. G. Peng and J. A. Neufeld, *Phys. Rev. Lett.*, 2013, **111**, 154501.
81 Z. Gu, S. Li, F. Zhang and S. Wang, *Adv. Sci.*, 2016, **3**, 1500327.
82 C. Creton and M. Ciccotti, *Rep. Prog. Phys.*, 2016, **79**, 046601.
83 C. Poulard, F. Restagno, R. Weil and L. Léger, *Soft Matter*, 2011, **7**, 2543–2551.
84 J. H. Ahn, H.-S. Kim, K. J. Lee, S. Jeon, S. J. Kang, Y. Sun, R. G. Nuzzo and J. A. Rogers, *Science*, 2006, **314**, 1754–1757.
85 X. Liang, Z. Fu and S. Y. Chou, *Nano Lett.*, 2007, **7**, 3840–3844.
86 K. Takei, T. Takahashi, J. C. Ho, H. Ko, A. G. Gillies, P. W. Leu, R. S. Fearing and A. Javey, *Nat. Mater.*, 2010, **9**, 821–826.
87 E. Ghavanloo, F. Daneshmand and M. Rafiei, *Phys. E*, 2010, **42**, 2218–2224.
88 B. Uğurlu, A. Kutlu, A. Ergin and M. Omurtag, *J. Sound Vib.*, 2008, **317**, 308–328.
89 D. Labonte, C. J. Clemente, A. Dittrich, C.-Y. Kuo, A. J. Crosby, D. J. Irschick and W. Federle, *Proc. Natl. Acad. Sci. U. S. A.*, 2016, **113**, 1297–1302.
90 J.-H. Dirks and W. Federle, *Soft Matter*, 2011, **7**, 11047–11053.
91 D. Labonte and W. Federle, *Soft Matter*, 2015, **11**, 8661–8673.
92 W. J. P. Barnes, P. J. P. Goodwyn, M. Nokhbatolfoghahai and S. N. Gorb, *J. Comp. Physiol., A*, 2011, **197**, 969.
93 M. D. Bartlett, A. B. Croll and A. J. Crosby, *Adv. Funct. Mater.*, 2012, **22**, 4985–4992.
94 M. D. Bartlett, A. B. Croll, D. R. King, B. M. Paret, D. J. Irschick and A. J. Crosby, *Adv. Mater.*, 2012, **24**, 1078–1083.
95 M. D. Bartlett and A. J. Crosby, *Langmuir*, 2013, **29**, 11022–11027.
96 D. R. King, M. D. Bartlett, C. A. Gilman, D. J. Irschick and A. J. Crosby, *Adv. Mater.*, 2014, **26**, 4345–4351.
97 A. R. Mojdehi, D. P. Holmes and D. A. Dillard, *Soft Matter*, 2017, **13**, 7529–7536.
98 W. Federle, W. Barnes, W. Baumgartner, P. Drechsler and J. Smith, *J. R. Soc., Interface*, 2006, **3**, 689–697.
99 C. Dhong and J. Frechette, *J. Appl. Phys.*, 2017, **121**, 044906.
100 J. A. Rogers, T. Someya and Y. Huang, *Science*, 2010, **327**, 1603–1607.
101 C. Michaut, *J. Geophys. Res.: Solid Earth*, 2011, **116**, B05205.
102 T. J. W. Wagner and D. Vella, *Phys. Rev. Lett.*, 2011, **107**, 044301.
103 Z. Zheng, I. M. Griffiths and H. A. Stone, *J. Fluid Mech.*, 2015, **784**, 443–464.
104 F. Boulogne, S. Khodaparast, C. Poulard and H. A. Stone, *Eur. Phys. J. E: Soft Matter Biol. Phys.*, 2017, **40**, 64.
105 C. Dhong and J. Fréchette, *Soft Matter*, 2015, **11**, 1901–1910.
106 R. D. Adams and N. A. Peppiatt, *J. Strain Anal. Eng. Des.*, 1974, **9**, 185–196.